

Chemistry of C-Trimethylsilyl-Substituted Heterocarboranes. 20. Synthetic and Structural Studies on Sandwich Ln(III) Carborane Clusters. II (Ln(III)) = Sm, Gd, Dy, Ho, Er

Narayan S. Hosmane,*† Ying Wang, Hongming Zhang, John A. Maguire,
Michael McInnis, Thomas G. Gray, and Jess D. Collins

Department of Chemistry, Southern Methodist University, Dallas, Texas 75275

Reinhard K. Kremer

Max-Planck-Institut für Festkörperforschung, Heisenbergstrasse 1, 70506 Stuttgart, Germany

Herbert Binder, Eberhard Waldhör, and Wolfgang Kaim

*Institut für Anorganische Chemie, Universität Stuttgart, Pfaffenwaldring 55,
70569 Stuttgart, Germany*

Received October 2, 1995‡

The room-temperature reactions of *closo-exo*-4,5-[$(\mu\text{-H})_2\text{Li}(\text{TMEDA})$]-1-Li(TMEDA)-2,3-($\text{SiMe}_3)_2$ -2,3-C₂B₄H₄ with anhydrous LnCl₃ (Ln = Sm, Gd, Dy, Ho, Er), in molar ratios of 2:1 in dry benzene (C₆H₆), produced the sandwich paramagnetic species [Li(TMEDA)₂][1-Cl-1-($\mu\text{-Cl}$)-2,2',3,3'-(SiMe_3)₂]-5,6-[$(\mu\text{-H})_2\text{Li}(\text{TMEDA})$]-4,4',5'-[$(\mu\text{-H})_3\text{Li}(\text{TMEDA})$]-1,1'-*commo*-Ln(2,3-C₂B₄H₄)₂] (Ln = Sm (**1**), Gd (**2**), Dy (**3**), Ho (**4**), Er (**5**)) in yields of 65%, 88%, 71%, 90%, and 93%, respectively. The compounds were characterized by IR spectroscopy, magnetic susceptibility measurements, and single-crystal X-ray diffraction studies. Compounds **2** and **3** were further characterized by EPR spectroscopy, and compound **1** was also characterized by ¹H, ¹³C, ¹¹B, and ⁷Li NMR spectroscopy. All compounds are bent-sandwich complexes in which a Ln(III) atom is coordinated to two carborane ligands and two chloride ions. The room-temperature magnetic susceptibilities of **1**–**4** were found to be 1.1, 7.3, 9.4, and 10.1 μ_B per metal atom, respectively.

Introduction

In the preceding paper in this series, we described the syntheses and characterizations of several trinuclear lanthanacarboranes of the C₂B₄ cage system having the general formula $\{\eta^5\text{-1-Ln-2,3-(SiMe}_3)_2\text{-2,3-C}_2\text{B}_4\text{H}_4\}_3[\mu_2\text{-1-Li-2,3-(SiMe}_3)_2\text{-2,3-C}_2\text{B}_4\text{H}_4\}_3(\mu_3\text{-OMe})][\mu_2\text{-Li}(\text{C}_4\text{H}_8\text{O})_3\text{-}(\mu_3\text{-O})]$ (Ln = Sm, Gd, Tb, Dy, Ho).^{1,2} These clusters were formed from the direct reaction of the THF-solvated dilithiacarborane *closo-exo*-4,5-Li(THF)₂-1-Li(THF)₂-2,3-(SiMe_3)₂-2,3-C₂B₄H₄ with the particular LnCl₃ salt in a dry benzene solution. The trinuclear clusters were found to be unreactive toward either additional LnCl₃ or dilithiacarborane; it was speculated that the formation of these clusters, rather than lanthanacarborane sandwich complexes, was dictated by the presence of the oxide ions MeO[−] and O^{2−} and that these ions were generated at some point in the reaction sequence. Since the reactions of THF with organolithium and with lanthanide compounds were well-documented,^{3,4} and the THF-solvated dilithiacarborane was known to degrade,⁵

the most probable source of the oxide ions was thought to be the THF molecules associated with the precursor dilithiacarboranes. In order to test this supposition, and to obtain more information on the role of the metal-solvating molecules on the course of the formation of the lanthanacarboranes, we have investigated the reaction of the TMEDA-solvated dilithiacarborane *closo-exo*-4,5-[$(\mu\text{-H})_2\text{Li}(\text{TMEDA})$]-1-Li(TMEDA)-2,3-(SiMe_3)₂-2,3-C₂B₄H₄ with LnCl₃ (Ln = Sm, Gd, Dy, Ho, Er), under reaction conditions equivalent to those used in the syntheses of the trinuclear lanthanacarborane clusters. Herein, we report the details of these investigations and the structures of the resulting lanthanide compounds, which proved to be quite different from those found in our previous study.¹

Experimental Section

Materials. Benzene, *N,N,N,N*-tetramethylethylenediamine (TMEDA), and *n*-hexane were dried over NaH and Na metal and doubly distilled before use. All other solvents were dried over 4–8 Å molecular sieves (Aldrich) and were either saturated with dry argon or degassed before use. The syn-

* Camille and Henry Dreyfus Scholar.

† Abstract published in *Advance ACS Abstracts*, January 15, 1996.

(1) Part 19: Hosmane, N. S.; Wang, Y.; Oki, A. R.; Zhang, H.; Maguire, J. A. *Organometallics* **1996**, *15*, 626.

(2) (a) Oki, A. R.; Zhang, H.; Hosmane, N. S. *Angew. Chem., Int. Ed. Engl.* **1992**, *31*, 432. (b) Zhang, H.; Oki, A. R.; Wang, Y.; Maguire, J. A.; Hosmane, N. S. *Acta Crystallogr., Cryst. Struct. Commun.* **1995**, *C51*, 635.

(3) (a) Jung, M. E.; Blum, R. B. *Tetrahedron Lett.* **1977**, 3791. (b) Maercker, A.; Theysohn, W. *Justus Liebigs Ann. Chem.* **1971**, *70*, 747. (c) Kamata, K.; Terashima, M. *Heterocycles* **1980**, *14*, 205.

(4) (a) Schumann, H.; Palamidis, E.; Loebel, J. *J. Organomet. Chem.* **1990**, *384*, C49–52. (b) Evans, W. J.; Grate, J. W.; Bloom, I.; Hunter, W. E.; Atwood, J. L. *J. Am. Chem. Soc.* **1985**, *107*, 405.

(5) Hosmane, N. S.; Saxena, A. K.; Barreto, R. D.; Maguire, J. A.; Jia, L.; Wang, Y.; Oki, A. R.; Grover, K. V.; Whitten, S. J.; Dawson, K.; Tolle, M. A.; Siriwardane, U.; Demissie, T.; Fagner, J. S. *Organometallics* **1993**, *12*, 3001.

(6) (a) Hosmane, N. S.; Sirmokadam, N. N.; Mollenhauer, M. N. *J. Organomet. Chem.* **1985**, *279*, 359. (b) Hosmane, N. S.; Mollenhauer, M. N.; Cowley, A. H.; Norman, N. C. *Organometallics* **1985**, *4*, 1194.

Table 1. Preparation of [Li(TMEDA)₂][1-Cl-1-(μ -Cl)-2,2',3,3'-(SiMe₃)₄-5,6-[(μ -H)₂Li(TMEDA)]-4,4',5'-[(μ -H)₃Li(TMEDA)]-1,1'-commo-Ln(2,3-C₂B₄H₄)₂]

compd	LnCl ₃ (amt; g, mmol)	amt of dilithiacarborane ^a (g, mmol)	color	mp (°C)	yield ^b (g, mmol, %)
1	SmCl ₃ (0.23, 0.9)	0.8, 1.7	yellow	185–187	0.63, 0.55, 65
2	GdCl ₃ (0.73, 2.78)	2.58, 5.56	colorless	165 dec	2.81, 2.45, 88
3	DyCl ₃ (1.05, 3.9)	3.62, 7.8	yellow	150	3.20, 2.78, 71
4	HoCl ₃ (0.66, 2.43)	2.26, 4.87	orange	>250	2.53, 2.19, 90
5	ErCl ₃ (0.87, 3.19)	2.96, 6.37	orange	>240	3.44, 2.97, 93

^a *clos*-*exo*-4,5-[(μ -H)₂Li(TMEDA)]-1-Li(TMEDA)-2,3-(SiMe₃)₂-2,3-C₂B₄H₄. ^b Yield is based on dilithiacarborane consumed.**Table 2. Infrared Absorptions (cm⁻¹, C₆H₆ vs C₆H₆)^a**

compd	abs
1	2957 (vs), 2896 (m), 2879 (w), 2840 (m), 2801 (m) [(CH)], 2532 (s), 2450 (m, br), 2364 (m) [ν (BH)], 1513 (w, br), 1456 (s), 1407 (m) [(CH)], 1356 (m), 1289 (m), 1256 (vs) [(CH)], 1166 (w), 1139 (w), 1099 (w), 1023 (m), 951 (m), 845 (vs) [(CH)], 795 (m), 761 (m), 639 (w), 589 (w)
2	2960 (vs), 2892 (m), 2874 (m), 2836 (s), 2792 (m) [(CH)], 2513 (s), 2463 (m, br), 2404 (m) [(BH)], 1550 (w, br), 1465 (vs), 1410 (w) [(CH)], 1387 (w), 1360 (w), 1247 (s) [(CH)], 1188 (m), 1159 (m), 1133 (m), 1104 (w), 1070 (m), 1024 (m), 945 (m), 840 (vs) [(CH)], 794 (m), 764 (m), 634 (m), 592 (w), 437 (m)
3	2963 (vs), 2893 (m), 2872 (m), 2837 (s), 2795 (s) [(CH)], 2517 (vs), 2468 (s), 2412 (m) [(BH)], 1552 (w, br), 1465 (s), 1409 (w) [(CH)], 1390 (w), 1361 (m), 1298 (s), 1250 (vs) [(CH)], 1186 (s), 1160 (m), 1138 (s), 1069 (m), 1027 (s), 957 (s), 846 (vs) [(CH)], 797 (s), 762 (m), 644 (m), 595 (w), 442 (m)
4	2959 (vs), 2901 (s), 2882 (s), 2837 (s), 2792 (s) [(CH)], 2515 (s), 2464 (m), 2406 (m) [(BH)], 1552 (w, br), 1508 (s), 1457 (vs), 1410 (m) [(CH)], 1391 (m), 1359 (m), 1299 (m), 1250 (s) [(CH)], 1192 (m), 1160 (m), 1140 (m), 1108 (m), 1070 (m), 1025 (m), 947 (s), 845 (vs) [(CH)], 780 (m), 768 (m), 639 (m), 593 (w)
5	2958 (vs), 2893 (m), 2873 (w), 2834 (m), 2793 (m) [(CH)], 2514 (s), 2465 (s), 2413 (m) [ν (BH)], 1479 (m), 1463 (s), 1444 (m) [(CH)], 1356 (m), 1289 (m), 1241 (vs) [(CH)], 1182 (m), 1159 (w), 1130 (m), 1099 (w), 1069 (w), 1036 (s), 1021 (m), 946 (s), 841 (vs) [(CH)], 793 (m), 760 (m), 680 (s), 633 (w), 590 (w)

^a Legend: v = very, s = strong or sharp, m = medium, w = weak, sh = shoulder, br = broad.**Table 3. Crystal Data^a for 1–5**

	1	2	3	4	5
formula	[C ₄₀ H ₁₀₈ N ₈ B ₈ Si ₄ Cl ₂ ·Li ₃ Sm]·0.5C ₆ H ₆	[C ₄₀ H ₁₀₈ N ₈ B ₈ Si ₄ Cl ₂ ·Li ₃ Gd]·0.5C ₆ H ₆	[C ₄₀ H ₁₀₈ N ₈ B ₈ Si ₄ Cl ₂ ·Li ₃ Dy]·0.5C ₆ H ₆	[C ₄₀ H ₁₀₈ N ₈ B ₈ Si ₄ Cl ₂ ·Li ₃ Ho]·0.5C ₆ H ₆	[C ₄₀ H ₁₀₈ N ₈ B ₈ Si ₄ Cl ₂ ·Li ₃ Er]·0.5C ₆ H ₆
fw	1181.3	1188.2	1193.5	1195.9	1198.2
space group	P ₂ ₁ /n	P ₂ ₁ 2 ₁ 2			
<i>a</i> , Å	14.830(4)	14.793(3)	14.679(2)	14.708(2)	21.051(6)
<i>b</i> , Å	21.196(6)	21.149(5)	21.062(4)	21.098(4)	23.435(6)
<i>c</i> , Å	23.215(4)	23.183(5)	23.068(4)	23.127(3)	14.148(4)
β , deg	93.20(2)	93.21(2)	93.17(1)	93.29(1)	90
<i>V</i> , Å ³	7286(3)	7242(3)	7121(2)	7165(2)	6980(3)
<i>Z</i>	4	4	4	4	4
<i>D</i> _{calcd.} , Mg/m ³	1.077	1.090	1.113	1.109	1.140
abs coeff, mm ⁻¹	0.976	1.087	1.223	1.277	1.380
crystal dmns, mm	0.30 × 0.20 × 0.10	0.15 × 0.35 × 0.10	0.25 × 0.10 × 0.05	0.30 × 0.15 × 0.05	0.10 × 0.15 × 0.25
scan type	ω	ω	θ	ω	ω
scan sp in ω , deg/min: min, max	6.0, 30.0	15.0, 30.0	6.0, 30.0	6.0, 30.0	6.0, 30.0
2θ range, deg	3.5–42.0	3.0–46.0	3.5–40.0	3.5–46.0	3.5–42.0
T, K	230	230	230	230	230
decay, %	0	0	0	0	0
no. of data collected	4259	10493	6981	10428	4166
no. of obsd rflns, <i>F</i> > 6.0σ(<i>F</i>)	2481	4835	3759 (<i>F</i> > 4.0σ(<i>F</i>))	8681 (<i>F</i> > 4.0σ(<i>F</i>))	2962
no. of params refined	314	623	622	623	455
GOF	1.23	1.08	0.99	0.99	1.68
Δρ(max, min), e/Å ³	0.58, -0.63	0.63, -0.52	0.56, -0.57	0.58, -0.30	1.48, -0.65
<i>R</i> ^b	0.055	0.048	0.055	0.050	0.056
<i>R</i> _w	0.063 ^c	0.055 ^c	0.057 ^c	0.092 ^d (wR2)	0.072

^a Graphite-monochromatized Mo Kα radiation, λ = 0.710 73 Å; ^b $R = \sum |F_0| - |F_c| / \sum |F_0|$, $R_w = [\sum w(F_0 - F_c)^2 / \sum w(F_0)^2]^{1/2}$; ^c $w = 1/\sigma^2(F_0) + 0.001(F_0)^2$; ^d $w = 1/\sigma^2(F_0^2) + (0.0437P^2)0.0P$, where $P = (F_0^2 + 2F_c^2)/3$.

thesis of 2,3-bis(trimethylsilyl)-2,3-dicarba-*nido*-hexaborane (8) and its subsequent conversion to *clos*-*exo*-4,5-[(μ -H)₂Li(TMEDA)]-1-Li(TMEDA)-2,3-(SiMe₃)₂-2,3-C₂B₄H₄ followed published procedures.^{5,6} Prior to use, SmCl₃, GdCl₃, DyCl₃, HoCl₃, and ErCl₃ (Strem) were degassed under vacuum at 130 °C for 24 h. *tert*-Butyllithium, *t*-BuLi (1.7 M solution in pentane, obtained from Aldrich), was used as received.

Spectroscopic Procedures. Proton, boron-11, carbon-13, and lithium-7 pulse Fourier transform NMR spectra, at 200, 64.2, 50.3, and 77.7 MHz, respectively, were recorded on an IBM-200 SY multinuclear NMR spectrometer. Infrared spec-

tra were recorded on a Perkin-Elmer Model 1600 FT-IR spectrophotometer or a Nicolet Magna 550 FT-IR spectrophotometer. Elemental analyses were determined by E + R Microanalytical Laboratory, Inc., Corona, NY.

Magnetic Susceptibility. Magnetic susceptibilities were measured with a MPMS Quantum Design SQUID magnetometer between 5 K and room temperature in a magnetic field of 1 T. The samples (~50 mg) were contained in gelatin capsules, the magnetizations of which were determined in separate runs and subtracted. Corrections for core diamagnetism were not applied.

**Table 4. Atomic Coordinates ($\times 10^4$) and Equivalent Isotropic Displacement Coefficients ($\text{\AA}^2 \times 10^3$)
(for 4 See Ref 14b)**

	<i>x</i>	<i>y</i>	<i>z</i>	<i>U</i> (eq)		<i>x</i>	<i>y</i>	<i>z</i>	<i>U</i> (eq)
Compound 1									
Sm	279(1)	2565(11)	8533(1)	32(3)	C(54)	-37(28)	-315(20)	7105(17)	152(14)
Cl(1)	460(3)	2902(3)	9614(2)	59(2)	C(55)	-249(23)	-385(17)	8678(14)	135(13)
Cl(2)	233(4)	3556(3)	7933(2)	55(2)	C(56)	-1495(17)	-111(14)	8060(12)	98(9)
Si(1)	2956(4)	2964(4)	8977(3)	57(2)	C(57)	319(22)	622(16)	6554(13)	125(12)
Si(2)	2290(4)	1253(3)	9417(3)	66(3)	C(58)	1451(20)	187(16)	7132(14)	130(12)
Si(3)	-2248(4)	3245(3)	8628(3)	61(3)	Li(2)	970(22)	3008(18)	7197(14)	49(9)
Si(4)	-1701(5)	1790(4)	9612(3)	66(3)	N(61)	74(15)	2957(12)	6406(9)	75(7)
C(11)	2155(10)	2385(13)	8624(7)	44(6)	N(62)	1859(13)	3502(10)	6701(8)	71(6)
C(12)	1847(14)	1719(12)	8784(9)	55(6)	C(63)	681(20)	3132(16)	6010(13)	122(11)
B(13)	1305(19)	1398(14)	8249(12)	64(8)	C(64)	1292(22)	3631(16)	6165(14)	127(12)
B(14)	1376(18)	1885(14)	7702(12)	58(8)	C(65)	-303(21)	2356(22)	6313(15)	156(19)
B(15)	1892(12)	2612(19)	7969(8)	46(7)	C(66)	-638(17)	3386(14)	6469(11)	96(9)
B(16)	2376(19)	1762(14)	8124(12)	65(8)	C(67)	2630(19)	3100(15)	6623(13)	128(12)
C(21)	-1572(9)	2567(25)	8493(6)	35(5)	C(68)	2133(23)	4066(16)	6951(14)	138(13)
C(22)	-1332(12)	1978(9)	8880(8)	36(5)	Li(3)	461(24)	3805(19)	11679(16)	57(10)
B(23)	-885(16)	1404(12)	8548(10)	42(7)	N(71)	-689(15)	4297(12)	11301(10)	91(7)
B(24)	-936(17)	1652(12)	7851(11)	49(7)	N(72)	257(21)	4340(16)	12442(14)	70(10)
B(25)	-1334(11)	2364(11)	7843(7)	29(6)	C(73)	-871(26)	4717(18)	11724(15)	145(14)
B(26)	-1919(20)	1820(14)	8247(13)	53(8)	C(74)	-689(23)	4576(18)	12328(14)	118(12)
C(31)	3229(14)	2856(11)	9772(8)	73(7)	C(75)	-1417(25)	3854(19)	11224(17)	171(16)
C(32)	2444(17)	3768(12)	8898(12)	78(8)	C(76)	-625(29)	4612(21)	10763(18)	204(20)
C(33)	4026(16)	2970(13)	8589(11)	100(10)	C(77)	221(20)	3917(15)	12960(13)	114(11)
C(34)	1941(17)	1555(13)	10130(10)	88(9)	C(78)	906(26)	4789(19)	12517(18)	163(16)
C(35)	3571(17)	1169(14)	9435(12)	105(10)	N(81)	1727(13)	3878(9)	11236(8)	80(6)
C(36)	1856(22)	427(15)	9391(14)	132(12)	N(82)	665(14)	2865(9)	11676(9)	88(7)
C(37)	-1657(15)	3812(11)	9155(9)	65(7)	C(83)	1870(23)	3165(16)	11205(14)	128(12)
C(38)	-3389(17)	3035(14)	8867(12)	103(10)	C(84)	1501(26)	2701(39)	11569(18)	265(28)
C(39)	-2427(17)	3702(13)	7968(10)	88(8)	C(85)	1641(19)	4173(14)	10682(10)	123(11)
C(40)	-1872(12)	2561(30)	10086(8)	85(8)	C(86)	2435(19)	4175(15)	11581(11)	138(13)
C(41)	-2770(16)	1310(13)	9555(11)	95(9)	C(87)	62(13)	2563(21)	11261(8)	96(7)
C(42)	-802(19)	1317(15)	10020(13)	118(11)	C(88)	620(19)	2561(23)	12223(10)	187(14)
Li(1)	-4(29)	792(23)	7881(18)	74(12)	C(91)	-7333(25)	291(23)	5011(7)	137(13)
N(51)	-483(14)	-142(11)	8109(10)	82(7)	C(92)	51(33)	622(11)	4875(17)	158(15)
N(52)	454(14)	279(11)	7086(9)	85(7)	C(93)	890(31)	309(26)	4897(20)	179(18)
C(53)	-91(44)	-543(29)	7689(22)	140(26)					
Compound 2									
Gd	283(1)	2432(1)	8521(1)	34(1)	C(54)	-82(13)	-301(9)	7100(9)	139(11)
Cl(1)	468(2)	2883(1)	9596(1)	59(1)	C(55)	-218(11)	-413(6)	8669(7)	125(8)
Cl(2)	232(2)	3548(1)	7942(1)	55(1)	C(56)	-1484(10)	-117(7)	8036(7)	106(8)
Si(1)	2956(2)	2966(2)	8973(1)	53(1)	C(57)	283(12)	611(9)	6551(7)	137(10)
Si(2)	2291(2)	1253(2)	9420(2)	66(1)	C(58)	1425(10)	190(8)	7159(7)	133(9)
Si(3)	-2235(2)	3242(2)	8637(2)	62(1)	Li(2)	932(14)	2980(10)	7195(8)	67(8)
Si(4)	-1682(3)	1792(2)	9615(2)	69(1)	N(61)	99(10)	2958(7)	6427(5)	95(6)
C(11)	2165(7)	2379(6)	8626(4)	50(4)	N(62)	1828(9)	3493(7)	6697(5)	89(6)
C(12)	1833(7)	1724(5)	8780(5)	47(4)	C(63)	683(13)	3177(11)	5986(6)	161(12)
B(13)	1332(10)	1395(7)	8251(6)	66(6)	C(64)	1323(12)	3639(10)	6174(8)	146(11)
B(14)	1379(10)	1887(7)	7708(6)	65(6)	C(65)	-319(13)	2360(9)	6306(6)	155(11)
B(15)	1909(7)	2527(7)	7975(5)	55(5)	C(66)	-652(12)	3389(10)	6458(7)	143(11)
B(16)	2400(10)	1776(8)	8152(7)	70(6)	C(67)	2619(12)	3119(11)	6593(7)	168(12)
C(21)	-1553(6)	2525(5)	8490(4)	43(3)	C(68)	2142(11)	4070(8)	6969(7)	131(9)
C(22)	-1303(6)	1978(5)	8882(4)	40(4)	Li(3)	486(12)	3833(9)	11659(9)	56(7)
B(23)	-882(8)	1434(5)	8546(5)	42(5)	N(71)	-708(8)	4271(6)	11321(7)	104(6)
B(24)	-932(8)	1652(6)	7861(6)	47(5)	N(72)	269(8)	4315(5)	12443(5)	75(5)
B(25)	-1315(8)	2380(6)	7847(5)	44(4)	C(73)	-850(13)	4764(9)	11171(12)	195(16)
B(26)	-1895(9)	1803(5)	8259(6)	44(5)	C(74)	-646(14)	4570(9)	12319(9)	158(12)
C(31)	3237(9)	2870(6)	9758(5)	79(5)	C(75)	-1424(11)	3878(8)	11231(9)	165(11)
C(32)	2438(8)	3772(5)	8902(5)	72(6)	C(76)	-638(15)	4590(11)	10775(10)	218(17)
C(33)	4033(8)	2965(7)	8597(6)	89(6)	C(77)	213(11)	3956(9)	12979(6)	126(9)
C(34)	1972(8)	1555(6)	10130(5)	82(6)	C(78)	912(14)	4777(9)	12559(9)	210(15)
C(35)	3540(9)	1167(7)	9412(6)	114(8)	N(81)	1704(7)	3893(6)	11236(5)	77(5)
C(36)	1834(11)	448(6)	9375(6)	126(8)	N(82)	659(9)	2852(5)	11695(5)	78(5)
C(37)	-1632(8)	3801(5)	9153(5)	80(6)	C(83)	1881(15)	3176(12)	11165(8)	162(13)
C(38)	-3388(8)	3051(8)	8863(6)	105(7)	C(84)	1576(17)	2806(10)	11577(12)	176(16)
C(39)	-2408(9)	3721(6)	7959(6)	96(6)	C(85)	1621(11)	4155(7)	10658(6)	114(8)
C(40)	-1865(9)	2489(6)	10092(5)	95(6)	C(86)	2413(11)	4210(11)	11574(7)	202(14)
C(41)	-2731(10)	1308(8)	9541(6)	121(8)	C(87)	70(11)	2516(7)	11292(6)	118(7)
C(42)	-801(10)	1309(6)	10003(5)	112(8)	C(88)	668(17)	2558(8)	12244(7)	193(14)
Li(1)	39(14)	779(10)	7857(10)	77(9)	C(91)	5770(20)	5300(25)	-10(10)	188(20)
N(51)	-491(8)	-161(5)	8107(5)	79(5)	C(92)	5005(32)	5631(8)	153(10)	204(17)
N(52)	478(9)	279(7)	7116(6)	102(6)	C(93)	4154(24)	5338(18)	110(11)	197(19)
C(53)	-128(15)	-577(8)	7676(9)	143(11)					

Table 4 (Continued)

	<i>x</i>	<i>y</i>	<i>z</i>	<i>U</i> (eq)		<i>x</i>	<i>y</i>	<i>z</i>	<i>U</i> (eq)
Compound 3									
Dy	286(1)	2416(1)	8512(1)	36(1)	C(54)	-93(16)	-298(11)	7081(10)	126(13)
Cl(1)	478(3)	2859(2)	9575(2)	55(2)	C(55)	-203(14)	-430(9)	8632(9)	125(12)
Cl(2)	233(3)	3536(2)	7962(2)	56(2)	C(56)	-1457(13)	-90(8)	8020(8)	103(10)
Si(1)	2953(3)	2959(2)	8965(2)	55(2)	C(57)	269(17)	613(12)	6546(10)	164(16)
Si(2)	2294(3)	1243(2)	9411(2)	65(2)	C(58)	1412(15)	172(9)	7151(9)	130(12)
Si(3)	-2219(3)	3242(2)	8654(2)	65(2)	Li(2)	929(19)	2974(12)	7205(11)	62(11)
Si(4)	-1652(3)	1782(3)	9616(2)	68(2)	N(61)	63(14)	2967(10)	6441(7)	106(9)
C(11)	2142(9)	2374(8)	8616(6)	42(6)	N(62)	1820(12)	3529(9)	6704(8)	91(8)
C(12)	1834(10)	1729(8)	8772(6)	44(6)	C(63)	619(17)	3188(14)	5989(9)	152(16)
B(13)	1319(11)	1406(9)	8250(9)	50(8)	C(64)	1280(18)	3638(14)	6182(10)	165(17)
B(14)	1375(11)	1885(10)	7718(8)	56(8)	C(65)	-324(16)	2358(10)	6294(8)	155(14)
B(15)	1891(10)	2527(9)	7969(7)	53(7)	C(66)	-688(16)	3403(11)	6482(8)	135(13)
B(16)	2384(13)	1775(10)	8156(9)	66(9)	C(67)	2571(15)	3141(12)	6591(8)	146(14)
C(21)	-1523(8)	2527(7)	8497(5)	32(5)	C(68)	2127(16)	4097(10)	6973(10)	157(15)
C(22)	-1295(9)	1979(7)	8885(6)	45(6)	Li(3)	479(16)	3828(11)	11683(12)	52(10)
B(23)	-881(11)	1434(8)	8524(8)	40(7)	N(71)	-732(12)	4267(9)	11327(10)	100(9)
B(24)	-901(11)	1673(8)	7863(7)	39(7)	N(72)	338(11)	4312(8)	12460(7)	76(7)
B(25)	-1305(11)	2380(9)	7860(8)	53(7)	C(73)	-908(19)	4647(17)	11822(18)	270(31)
B(26)	-1899(11)	1801(8)	8250(8)	48(7)	C(74)	-530(23)	4638(13)	12348(12)	156(19)
C(31)	3231(11)	2849(7)	9767(6)	73(7)	C(75)	-1453(14)	3851(10)	11236(11)	162(15)
C(32)	2427(10)	3756(7)	8899(7)	70(8)	C(76)	-636(20)	4630(15)	10866(15)	268(30)
C(33)	4029(9)	2938(8)	8583(7)	83(8)	C(77)	237(13)	3953(10)	12963(8)	117(11)
C(34)	1971(11)	1541(8)	10117(6)	79(8)	C(78)	1004(19)	4780(11)	12565(11)	214(19)
C(35)	3551(11)	1178(9)	9414(8)	116(10)	N(81)	1672(11)	3909(9)	11212(8)	78(7)
C(36)	1815(14)	444(8)	9365(8)	130(12)	N(82)	673(14)	2858(7)	11683(8)	81(7)
C(37)	-1608(11)	3787(7)	9172(7)	88(8)	C(83)	1904(17)	3219(17)	11167(10)	141(17)
C(38)	-3352(10)	3030(9)	8901(8)	107(10)	C(84)	1546(23)	2801(13)	11537(17)	199(25)
C(39)	-2420(12)	3703(7)	7988(7)	95(9)	C(85)	1605(15)	4150(10)	10657(10)	134(13)
C(40)	-1825(12)	2485(8)	10103(6)	98(8)	C(86)	2393(14)	4223(12)	11557(9)	187(17)
C(41)	-2711(12)	1309(9)	9556(8)	117(11)	C(87)	83(14)	2508(9)	11293(8)	125(10)
C(42)	-771(12)	1314(8)	10012(7)	100(9)	C(88)	702(21)	2572(10)	12231(11)	212(20)
Li(1)	67(19)	787(12)	7860(12)	64(11)	C(91)	5797(26)	5292(31)	-11(12)	142(20)
N(51)	-498(11)	-166(7)	8089(9)	90(8)	C(92)	5020(49)	5648(15)	128(12)	163(18)
N(52)	453(13)	285(9)	7090(9)	99(9)	C(93)	4170(32)	5330(25)	137(13)	180(23)
C(53)	-133(16)	-588(9)	7649(10)	116(12)					
Compound 5									
Er	7308(1)	3550(1)	2452(1)	38(1)	C(54)	4716(10)	1974(10)	2557(27)	85(10)
Cl(1)	7692(3)	4589(2)	2663(4)	57(2)	C(55)	4452(10)	3517(11)	2502(28)	134(16)
Cl(2)	8451(3)	3078(2)	2238(5)	66(3)	C(56)	4681(13)	2954(17)	1034(17)	147(20)
Si(1)	8011(4)	3945(4)	5110(6)	62(3)	C(57)	5693(12)	1512(10)	2748(23)	94(13)
Si(2)	6236(4)	4284(3)	4724(6)	73(3)	C(58)	5294(15)	2028(12)	3971(21)	110(16)
Si(3)	7884(4)	3954(4)	-246(6)	66(3)	Li(2)	7995(15)	2247(13)	3009(22)	40(8)
Si(4)	6417(4)	4723(4)	693(6)	76(3)	N(61)	7990(8)	1561(5)	2062(11)	99(10)
C(11)	7407(11)	3590(10)	4329(14)	48(6)	N(62)	8437(9)	1701(7)	4047(13)	106(13)
C(12)	6707(10)	3729(9)	4123(14)	36(6)	C(63)	8200(12)	1052(8)	2610(16)	144(18)
B(13)	6399(13)	3201(11)	3688(16)	42(7)	C(64)	8652(12)	1209(10)	3462(13)	205(27)
B(14)	6934(12)	2710(10)	3590(17)	43(6)	C(65)	7363(9)	1439(9)	1618(17)	115(14)
B(15)	7569(13)	2988(10)	4044(16)	46(7)	C(66)	8464(10)	1684(10)	1306(16)	107(15)
B(16)	6815(12)	3106(11)	4703(19)	48(7)	C(67)	7931(12)	1505(10)	4710(20)	151(19)
C(21)	7278(12)	3667(10)	565(14)	47(6)	C(68)	8985(12)	1923(12)	4603(22)	199(26)
C(22)	6722(10)	3993(10)	933(15)	48(6)	Li(3)	1060(8)	3347(7)	2060(13)	82(14)
B(23)	6224(13)	3572(12)	1434(18)	56(7)	N(71)	1997(9)	3119(9)	2155(16)	145(11)
B(24)	6533(13)	2932(12)	1274(17)	48(7)	N(72)	725(10)	2602(8)	2633(18)	153(10)
B(25)	7215(14)	3014(12)	730(18)	59(8)	C(73)	1832(13)	2501(11)	2176(27)	398(43)
B(26)	6566(12)	3428(10)	354(19)	48(7)	C(74)	1355(9)	2440(20)	3032(24)	806(113)
C(31)	7879(11)	4753(10)	5418(19)	86(12)	C(75)	2366(14)	3243(11)	1279(16)	99(9)
C(32)	8789(11)	3873(10)	4538(18)	79(11)	C(76)	2393(22)	3260(19)	2996(17)	318(35)
C(33)	8054(14)	3547(12)	6292(15)	90(12)	C(77)	233(13)	2553(15)	3385(23)	159(15)
C(34)	6389(13)	5027(10)	4288(21)	94(13)	C(78)	564(19)	2208(20)	1843(25)	303(34)
C(35)	6257(19)	4254(13)	5983(26)	202(26)	N(81)	648(10)	3750(8)	932(12)	99(8)
C(36)	5401(11)	4154(10)	4472(26)	127(17)	N(82)	755(15)	4046(9)	2800(18)	407(36)
C(37)	8431(14)	4451(12)	364(19)	114(14)	C(83)	391(12)	4314(10)	1233(18)	212(21)
C(38)	7544(12)	4282(14)	-1308(18)	105(14)	C(84)	833(16)	4503(11)	2078(16)	222(22)
C(39)	8388(13)	3379(12)	-612(19)	98(13)	C(85)	1149(14)	3841(14)	202(25)	201(19)
C(40)	7006(12)	5299(9)	548(18)	84(11)	C(86)	125(14)	3402(14)	518(30)	262(26)
C(41)	5865(16)	4733(14)	-400(2)	147(19)	C(87)	96(16)	4066(18)	3182(22)	202(19)
C(42)	5939(14)	4961(11)	1621(23)	128(16)	C(88)	1214(19)	4144(21)	3586(29)	285(30)
Li(1)	5695(18)	2767(16)	2504(47)	80(11)	C(91)	5243(15)	-78(18)	1477(21)	124(13)
N(51)	4709(9)	2957(10)	2082(18)	88(11)	C(92)	5630(13)	-162(12)	2285(16)	105(9)
N(52)	5329(9)	2009(9)	2950(14)	64(8)	C(93)	5390(15)	-125(16)	3219(21)	112(11)
C(53)	4357(9)	2506(9)	2515(29)	77(9)					

^a Equivalent isotropic *U*, defined as one-third of the trace of the orthogonalized \mathbf{U}_{ij} tensor.

EPR Spectra. Measurements were made on a Bruker ESP 300 in the X-band mode, equipped with a Bruker ER035M gauss meter, an HP 5350B microwave counter, and an Oxford Instruments ESP 900 cryostat.

Synthetic Procedures. All experiments were carried out in Pyrex glass round-bottom flasks of 100 mL capacity, equipped with magnetic stirring bars and high-vacuum Teflon valves. After their initial purifications, nonvolatile substances were manipulated in either a drybox or an evacuable glovebag, under an atmosphere of dry nitrogen. All known compounds among the products were identified by comparing their IR and ^1H NMR spectra with those of authentic samples.

Synthesis of $[\text{Li}(\text{TMEDA})_2][1\text{-Cl-1-(}\mu\text{-Cl)-2,2',3,3'-(SiMe}_3)_4\text{5,6-}[(\mu\text{-H})_2\text{Li(TMEDA)}]\text{-4,4',5'-}[(\mu\text{-H})_3\text{Li(TMEDA)}]\text{-1,1'-commo-Ln(2,3-C}_2\text{B}_4\text{H}_4)_2]$ (Ln = Sm (1), Gd (2), Dy (3), Ho (4), Er (5)). Except for the quantities used, the procedures in the synthesis of compounds **1–5** were identical. Therefore, only a typical synthesis will be described; the details of quantities used, product yields, and certain physical properties of **1–5** are summarized in Table 1.

A previously weighed sample of *clos-o-exo*-4,5- $[(\mu\text{-H})_2\text{Li(TMEDA)}]\text{-1-Li(TMEDA)-2,3-(SiMe}_3)_2\text{-2,3-C}_2\text{B}_4\text{H}_4$ was reacted with anhydrous LnCl_3 , in a molar ratio of 2:1, in about 30 mL of dry benzene, with constant stirring, at 0 °C for 2–3 h and then at room temperature for an additional 36 h. During this period the solution became turbid and turned orange. The heterogeneous product mixture was then filtered through a frit, and the residue was washed repeatedly with anhydrous benzene. The solid that remained on the frit after repeated washings was identified by qualitative analysis as LiCl (not measured) and was discarded. Slow evaporation of the solvent from the filtrate yielded air-sensitive crystalline solids identified as $[\text{Li}(\text{TMEDA})_2][1\text{-Cl-1-(}\mu\text{-Cl)-2,2',3,3'-(SiMe}_3)_4\text{5,6-}[(\mu\text{-H})_2\text{Li(TMEDA)}]\text{-4,4',5'-}[(\mu\text{-H})_3\text{Li(TMEDA)}]\text{-1,1'-commo-Ln(2,3-C}_2\text{B}_4\text{H}_4)_2]$ (Ln = Sm (**1**), Gd (**2**), Dy (**3**), Ho (**4**), Er (**5**)). Anal. Calcd (found) for $\text{C}_{40}\text{H}_{108}\text{B}_8\text{Cl}_2\text{N}_8\text{Si}_4\text{Li}_3\text{Sm}$ (**1**): C, 42.1 (41.91); H, 9.53 (9.36); N, 9.81 (9.49). Calcd (found) for $\text{C}_{40}\text{H}_{108}\text{B}_8\text{Cl}_2\text{N}_8\text{Si}_4\text{Li}_3\text{Gd}$ (**2**): C, 41.8 (41.58); H, 9.47 (9.34); N, 9.75 (9.58). Calcd (found) for $\text{C}_{40}\text{H}_{108}\text{B}_8\text{Cl}_2\text{N}_8\text{Si}_4\text{Li}_3\text{Dy}$ (**3**): C, 41.6 (41.88); H, 9.43 (9.25); N, 9.71 (9.51). Calcd (found) for $\text{C}_{40}\text{H}_{108}\text{B}_8\text{Cl}_2\text{N}_8\text{Si}_4\text{Li}_3\text{Ho}$ (**4**): C, 41.50 (41.61); H, 9.41 (9.43); N, 9.69 (9.55). Calcd (found) for $\text{C}_{40}\text{H}_{108}\text{B}_8\text{Cl}_2\text{N}_8\text{Si}_4\text{Li}_3\text{Er}$ (**5**): C, 41.50 (41.5); H, 9.39 (9.18); N, 9.67 (9.46). The infrared spectral data with selected assignments for **1–5** are presented in Table 2. NMR data for complex **1**: ^1H NMR ($\text{C}_4\text{D}_8\text{O}$, external Me_4Si) δ 2.4 [s, CH_2 , TMEDA], 2.3 [s, CH_3 , TMEDA], 0.74 [s, $\text{Si}(\text{CH}_3)_3$]; ^{11}B NMR ($\text{C}_4\text{D}_8\text{O}$, external $\text{BF}_3\cdot\text{OEt}_2$) δ 13.7 [br, ill-defined peak, 2B, basal BH, $^1J(^{11}\text{B}-^1\text{H})$ unresolved], -2.8 [br, ill-defined peak, 1B, basal BH, $^1J(^{11}\text{B}-^1\text{H})$ unresolved], -21.6 [br, ill-defined peak, 1B, apical BH, $^1J(^{11}\text{B}-^1\text{H})$ unresolved]; ^{13}C NMR (C_6D_6 , external Me_4Si) δ 96.9 [s (v br), cage carbons (SiCB)], 57.1 [t, TMEDA, $^1J(^{13}\text{C}-^1\text{H})$ = 137.5 Hz], 46.1 [q, TMEDA, $^1J(^{13}\text{C}-^1\text{H})$ = 135.4 Hz], 3.5 [q, SiMe_3 , $^1J(^{13}\text{C}-^1\text{H})$ = 120.3 Hz]; ^{7}Li NMR (C_6D_6 , external aqueous LiNO_3) δ -1.2 (br) ppm. The paramagnetism of **2–5** did not allow the recording of useful NMR spectra for these compounds.

Crystal Structure Analysis of **1–5.** Crystals of the particular lanthanacarborane were grown from a hexane/benzene (40/60 v/v) solution by slow evaporation. The crystals were then mounted on a Siemens R3m/V diffractometer, under a low-temperature nitrogen stream. The pertinent crystallographic data for **1–5** are summarized in Table 3. Final unit cell parameters were obtained by a least-squares fit of the angles of 24–30 accurately centered reflections in the 2θ range from 18 to 32°. Compounds **1–4** were found to be isostructural. Their space groups were uniquely determined from systematic absences as P_{2_1}/c , while the systematic absences in **5** were consistent with the space group $P_{2_1}2_12$. Intensity data for compounds **1–5** were collected at 230 K. For each compound, three standard reflections were monitored during the data collection and did not show any significant change in intensities. All data sets were corrected for Lorentz and

polarization effects; semiempirical absorption studies (ψ scans) were applied for each structure. All structures were solved by heavy-atom methods and subsequent difference Fourier syntheses using the SHELXTL-Plus package.⁷ The structure of **4** was refined on F^2 for all reflections using SHELXL93.⁸ Weighted R_w and goodness-of-fit values were based on F^2 , while the conventional R factor was based on F , with F set equal to zero for negative values of F^2 . The observed criterion of $F > 4.0\sigma(F)$ was used only for the R -factor calculation; it was not relevant to the choice of reflections for refinement. All other structures were refined on F using SHELXTL-Plus.⁷ The criteria used to choose reflections for refinement were $F > 6.0\sigma(F)$ for structures **1**, **2**, and **5** and $F > 4.0\sigma(F)$ for structure **3**. Scattering factors, with corrections for anomalous dispersion of lanthanide elements and Cl atoms, were taken from ref 9. A benzene half-molecule of solvation was present in each structure. In structures **1–4** the geometrical center of the benzene molecule was located at the symmetrical center of the structure. In structure **5**, the benzene possessed a 2-fold symmetry whose symmetrical axis was parallel to the crystallographic *b* axis and passed through the midpoints of $\text{C}(91)-\text{C}(93)^i$ and $\text{C}(93)-\text{C}(91)^i$ ($i = -x, y, -z$). Full-matrix refinement was performed for each structure. In structures **2–4**, all non-H atoms were anisotropically refined. The Sm, Cl, and Si atoms in structure **1** and the Er, Cl, Si, methyl C, and N and C atoms of nondisordered TMEDA in structure **5** were refined anisotropically. The solvated benzenes and some of the TMEDA ligands of the $\text{Li}^+(\text{TMEDA})_2$ cations were disordered and were elastically restrained in the final stages of refinement. The carborane-cage H atoms of **2–5** were located in ΔF maps. Methyl and methylene H's of all five structures were calculated using a riding model. In structures **1**, **2**, **3**, and **5** the isotropic displacement parameters of all H atoms were set at $U = 0.08 \text{ \AA}^2$, while those of structure **4** were assigned to $1.50 U_{eq}$ of the attached C and B atoms. The final values of R and weighted R_w are listed in Table 3. For all structures $R = \sum ||F_o| - |F_c|| / \sum |F_o|$. For **1**, **2**, **3**, and **5**, $R_w = [\sum w(|F_o| - |F_c|)^2 / \sum w(F_o)^2]^{1/2}$ ($w = [\sigma^2(F) + 0.001(F^2)]^{-1}$), while for **4** the weight had the form $w = 1/[\sigma^2(F^2) + 0.0437P^2]$, where $P = (F_o^2 + 2F_c^2)/3$. The atomic coordinates are given in Table 4, while selected interatomic distances and angles are listed in Table 5.

Results and Discussion

Synthesis. The room-temperature reactions of *clos-o*-4,5- $[(\mu\text{-H})_2\text{Li(TMEDA)}]\text{-1-Li(TMEDA)-2,3-(SiMe}_3)_2\text{-2,3-C}_2\text{B}_4\text{H}_4$ with anhydrous LnCl_3 (Ln = Sm, Gd, Dy, Ho, Er), in molar ratios of 2:1 in dry benzene (C_6H_6) solutions, produced the sandwich species $[\text{Li}(\text{TMEDA})_2][1\text{-Cl-1-(}\mu\text{-Cl)-2,2',3,3'-(SiMe}_3)_4\text{5,6-}[(\mu\text{-H})_2\text{Li(TMEDA)}]\text{-4,4',5'-}[(\mu\text{-H})_3\text{Li(TMEDA)}]\text{-1,1'-commo-Ln(2,3-C}_2\text{B}_4\text{H}_4)_2]$ (Ln = Sm (**1**), Gd (**2**), Dy (**3**), Ho (**4**), Er (**5**)) in yields of 65, 88, 71, 90, and 93%, respectively, as outlined in Scheme 1. The results of these reactions differ greatly from those obtained when the THF-solvated dilithiacarborane was used, in which the only identifiable products were trinuclear clusters of the half-sandwich lanthanacarboranes and excess dilithiacarboranes.¹ These results tend to confirm the earlier speculation that the oxide ions, presumably produced by the degradation of the THF molecules, stabilized the cluster of the half-sandwich complexes to the extent that

(7) Sheldrick, G. M. Structure Determination Software Programs; Siemens X-ray Analytical Instruments Corp., Madison, WI, 1990.

(8) Sheldrick, G. M. SHELXL93, Program for the Refinement of Crystal Structures; University of Göttingen, Göttingen, Germany, 1993.

(9) International Tables For X-ray Crystallography; Kynoch Press: Birmingham, U.K., 1974; Vol. IV.

Table 5. Selected Interatomic Distances (\AA) and Angles (deg)^a

Interatomic Distances							
Compound 1							
Sm–Cnt(1)	2.551	Sm–Cnt(2)	2.544	Sm–B(15)	2.793(19)	Sm–C(21)	2.741(13)
Sm–Cl(1)	2.609(8)	Sm–Cl(2)	2.520(21)	Sm–C(22)	2.849(21)	Sm–B(23)	3.007(31)
Sm–C(11)	2.805(16)	Sm–C(12)	2.968(27)	Sm–B(24)	3.029(29)	Sm–B(25)	2.836(17)
Sm–B(13)	2.997(36)	Sm–B(14)	2.968(30)	Cl(2)–Li(2)	2.381(35)		
Compound 2							
Gd–Cnt(3)	2.435	Gd–Cnt(4)	2.397	Gd–B(15)	2.788(11)	Gd–C(21)	2.720(8)
Gd–Cl(1)	2.667(3)	Gd–Cl(2)	2.714(3)	Gd–C(22)	2.711(10)	Gd–B(23)	2.728(12)
Gd–C(11)	2.783(10)	Gd–C(12)	2.775(10)	Gd–B(24)	2.825(12)	Gd–B(25)	2.763(11)
Gd–B(13)	2.777(15)	Gd–B(14)	2.802(15)	Cl(2)–Li(2)	2.390(20)		
Compound 3							
Dy–Cnt(5)	2.380	Dy–Cnt(6)	2.344	Dy–B(15)	2.739(16)	Dy–C(21)	2.665(11)
Dy–Cl(1)	2.622(4)	Dy–Cl(2)	2.678(4)	Dy–C(22)	2.683(14)	Dy–B(23)	2.687(17)
Dy–C(11)	2.723(13)	Dy–C(12)	2.731(15)	Dy–B(24)	2.727(16)	Dy–B(25)	2.710(16)
Dy–B(13)	2.700(18)	Dy–B(14)	2.736(19)	Cl(2)–Li(2)	2.386(27)		
Compound 4							
Ho–Cnt(7)	2.378	Ho–Cnt(8)	2.350	Ho–B(15)	2.714(8)	Ho–C(21)	2.670(6)
Ho–Cl(1)	2.613(2)	Ho–Cl(2)	2.669(2)	Ho–C(22)	2.670(7)	Ho–B(23)	2.695(8)
Ho–C(11)	2.723(6)	Ho–C(12)	2.752(7)	Ho–B(24)	2.767(8)	Ho–B(25)	2.713(7)
Ho–B(13)	2.722(8)	Ho–B(14)	2.751(9)	Cl(2)–Li(2)	2.360(14)		
Compound 5							
Er–Cnt(9)	2.334	Er–Cnt(10)	2.353	Er–B(15)	2.666(24)	Er–C(21)	2.685(19)
Er–Cl(1)	2.583(5)	Er–Cl(2)	2.665(5)	Er–C(22)	2.686(22)	Er–B(23)	2.700(27)
Er–C(11)	2.665(19)	Er–C(12)	2.715(20)	Er–B(24)	2.746(27)	Er–B(25)	2.749(26)
Er–B(13)	2.717(25)	Er–B(14)	2.662(24)	Cl(2)–Li(2)	2.429(32)		
Interatomic Angles							
Compound 1							
Cnt(1)–Sm–Cl(1)	108.7	Cnt(1)–Sm–Cl(2)	104.7	Cnt(1)–Sm–Cnt(2)	117.3	Cl(1)–Sm–Cl(2)	107.6(8)
Cnt(2)–Sm–Cl(1)	110.9	Cnt(2)–Sm–Cl(2)	107.1	Sm–Cl(2)–Li(2)	89.5(9)		
Compound 2							
Cnt(3)–Gd–Cl(1)	108.7	Cnt(3)–Gd–Cl(2)	102.7	Cnt(3)–Gd–Cnt(4)	127.3	Cl(1)–Gd–Cl(2)	98.6(1)
Cnt(4)–Gd–Cl(1)	111.1	Cnt(4)–Gd–Cl(2)	104.0	Gd–Cl(2)–Li(2)	85.4(5)		
Compound 3							
Cnt(5)–Dy–Cl(1)	108.0	Cnt(5)–Dy–Cl(2)	103.0	Cnt(5)–Dy–Cnt(6)	128.6	Cl(1)–Dy–Cl(2)	97.4(1)
Cnt(6)–Dy–Cl(1)	110.8	Cnt(6)–Dy–Cl(2)	103.9	Dy–Cl(2)–Li(2)	84.7(6)		
Compound 4							
Cnt(7)–Ho–Cl(1)	107.9	Cnt(7)–Ho–Cl(2)	103.2	Cnt(7)–Ho–Cnt(8)	128.5	Cl(1)–Ho–Cl(2)	97.17(6)
Cnt(8)–Ho–Cl(1)	110.6	Cnt(8)–Ho–Cl(2)	104.4	Li(2)–Cl(2)–Ho	84.7(3)		
Compound 5							
Cnt(9)–Er–Cl(1)	105.7	Cnt(9)–Er–Cl(2)	103.0	Cnt(9)–Er–Cnt(10)	129.8	Cl(1)–Er–Cl(2)	97.0(2)
Cnt(10)–Er–Cl(1)	110.7	Cnt(10)–Er–Cl(2)	105.5	Er–Cl(2)–Li(2)	85.7(8)		

^a Legend: Cnt(1) and Cnt(2), the centroids of C_2B_3 rings of compound 1; Cnt(3) and Cnt(4), the centroids of C_2B_3 rings of compound 2; ..., Cnt(9) and Cnt(10), the centroids of C_2B_3 rings of compound 5.

the lanthanacarborane syntheses were effectively terminated at that stage. In the absence of the oxygen-containing THF molecules, the reactions led to the formation of the expected full-sandwich lanthanacarboranes, similar to those found in the larger C_2B_9 cage system.^{10–12}

Crystal Structures. The structures of compounds 1–5 are all quite similar. Therefore, only the structure of the gadolinacarborane (2) is shown in Figure 1; the ORTEP drawings of compounds 1, 3, 4, and 5 are given in the Supporting Information. Figure 2 shows the unit cell diagram for compound 2, which is typical of the lanthanacarboranes. The packing diagram clearly shows that the $\text{Li}^+(\text{TMEDA})_2$ cationic unit is well-separated from the lanthanacarborane monoanion. Figure 1 shows that in these anions the Ln(III) metals are sandwiched between two carborane cages and are also coordinated by two chloride ions. The various ligand–

(10) Fronczek, F. R.; Halstead, G. W.; Raymond, K. N. *J. Am. Chem. Soc.* **1977**, *99*, 1769.

(11) Manning, M. J.; Knobler, C. B.; Hawthorne, M. F. *J. Am. Chem. Soc.* **1988**, *110*, 4458.

(12) Manning, M. J.; Knobler, C. B.; Khattar, R.; Hawthorne, M. F. *Inorg. Chem.* **1991**, *30*, 2009.

Ln–ligand angles, given in Table 5, indicate a distorted-tetrahedral arrangement around the lanthanide metals. These structures are also quite similar to those found for other $(\text{CB})_2\text{LnX}_2$ carborane (CB) complexes^{10–14} and the early d-group metallocenes of the type Cp_2MX_2 .¹⁵ Excluding the samaracarborane (1), the average Cnt–Ln–Cnt angle is $128.6 \pm 0.6^\circ$,¹⁶ which is very close to the value of 129.7° found in both $\{\text{Y}(\text{Cl})(\text{THF})[\eta^5\text{(SiMe}_3)_2\text{C}_2\text{B}_4\text{H}_4]_2\}^{2-}$ and $\{\text{Er}(\text{Cl})_2[\eta^5\text{(SiMe}_3)_2\text{C}_2\text{B}_4\text{H}_4]_2\}^{3-}$ ^{13,14a} but less than the values of 137° found in $\{\text{U}(\text{Cl})_2[\eta^5\text{-C}_2\text{B}_9\text{H}_{11}]_2\}^{2-}$ and 131.9° reported for $\{\text{Sm}(\text{THF})_2[\eta^5\text{-C}_2\text{B}_9\text{H}_{11}]_2\}^-$.^{10–12} The Ln– C_2B_3 –atom distances in 2–4 are very similar to the analogous values found in the corresponding trinuclear clusters of these metals; the average Ln–Cnt distances in the trinuclear

(13) Oki, A. R.; Zhang, H.; Hosmane, N. S. *Organometallics* **1991**, *10*, 3964.

(14) (a) Hosmane, N. S.; Wang, Y.; Zhang, H.; Oki, A. R.; Maguire, J. A.; Waldhör, E.; Kaim, W.; Binder, H.; Kremer, R. K. *Organometallics* **1995**, *14*, 1101. (b) Zhang, H.; Wang, Y.; Maguire, J. A.; Hosmane, N. S. *Acta Crystallogr., Cryst. Struct. Commun.*, in press.

(15) Prout, K.; Cameron, T. S.; Forder, R. A.; Critchley, S. R.; Denton, B.; Rees, G. V. *Acta Crystallogr., Sect. B* **1974**, *30*, 2290.

(16) When an average value of a variable is given, the uncertainty quoted is the average deviation.

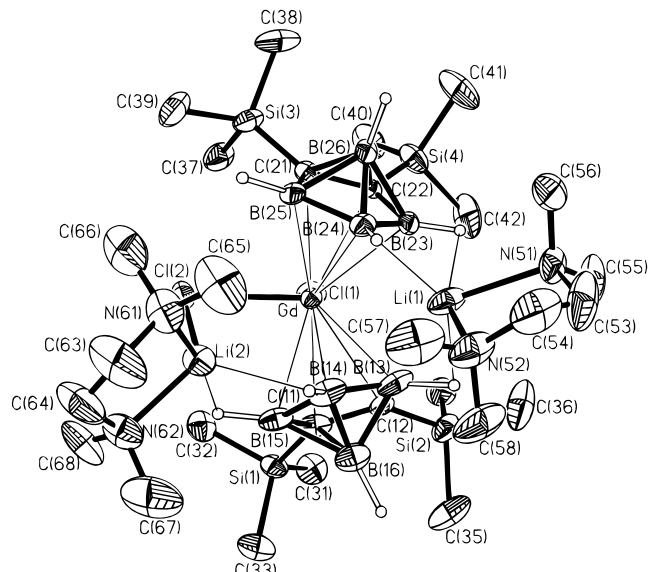
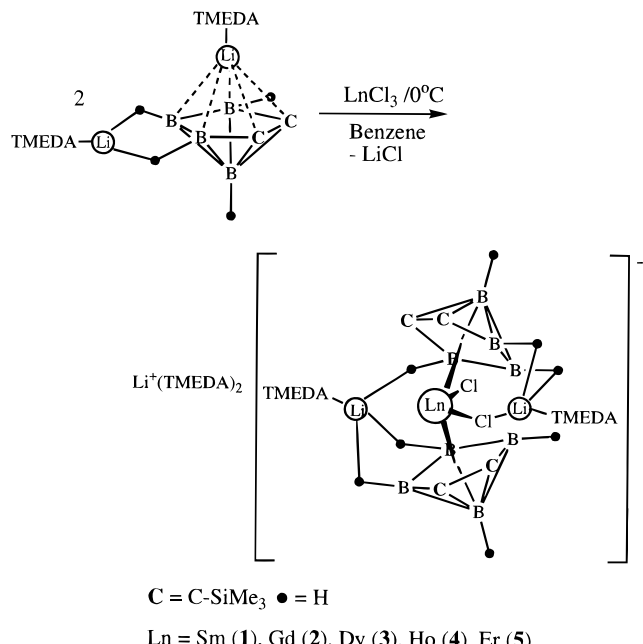


Figure 1. Perspective view of **2** showing the atom-numbering scheme, with thermal ellipsoids drawn at the 40% probability level. The methyl and methylene H atoms and the exo-polyhedral $\text{Li}^+(\text{TMEDA})_2$ cation are omitted for clarity.

Scheme 1



clusters of Gd, Dy, and Ho are 2.393 ± 0.008 , 2.356 ± 0.020 , and 2.342 ± 0.010 Å, respectively,¹ which are close to the values found for the sandwich compounds (see Table 5). The decreases in the various metal–ligand bond distances found in going from **2** to **5** are those expected from the decrease in the metals' ionic radii, suggesting essentially electrostatic metal–carborane interactions. This was the same conclusion reached in the case of the analogous trinuclear complexes.¹ Since the interatom distances and angles in the samaracarborane (**1**) differ significantly from what one would expect by extrapolation from the other lanthanacarboranes, it was excluded from the above comparisons. The bond distances in **1**, listed in Table 5, indicate that the Sm does not bond symmetrically to the C_2B_3 face of the carborane involving $\text{C}(11)$ – $\text{B}(15)$ but is slipped toward

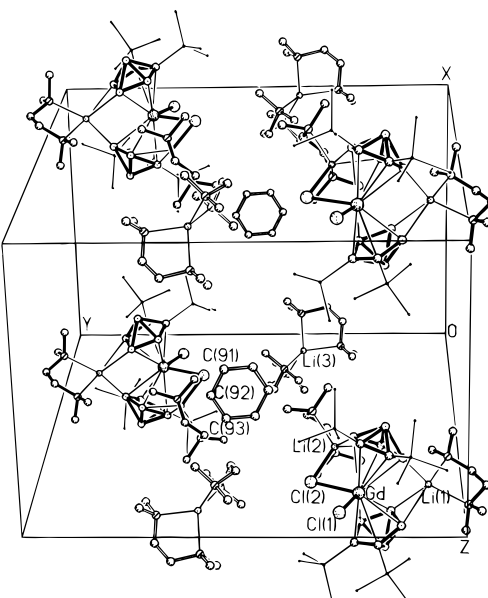


Figure 2. Crystal packing diagram of **2**.

$\text{C}(11)$ and $\text{B}(15)$. This slippage is not found for the other carborane cage, nor is it reflected in the other lanthanacarboranes contained in this study. This apparent distortion is probably the result of problems encountered in the X-ray crystal structure determination of **1** (see Experimental Section), rather than a reflection of any inherent metal–ligand bonding preferences. Nevertheless, the dislocation of the Sm from the centroidal position above the carborane face does affect the values of several other important geometric parameters given in Table 5. Specifically, there are larger than expected Sm–Cnt distances and an unusually small Cnt–Sm–Cnt bond angle, 117.3° for **1** compared to $128.6 \pm 0.6^\circ$ found for **2**–**5**. An alternate way to gauge the extent of bending of a sandwich compound involving two planar ligand faces is to measure the dihedral angle of the faces. The dihedral angles between the two C_2B_3 faces in **1**–**5** are 51.2 , 51.9 , 51.8 , 50.8 , and 49.8° , respectively. For a metal symmetrically bound to such planar cyclic ligands, these dihedral angles and the Cnt–M–Cnt angles should add up to 180° . This is what is found for all the compounds except **1**. In view of the limitations imposed by the accuracy of the X-ray analysis, all of the complexes seem to have very similar structures, and any changes in the geometric parameters that are found in these lanthanide sandwich complexes can be related to the variation in the size of the lanthanide metals.

Spectroscopy. Compounds **1**–**5** were also characterized by IR spectroscopy and by elemental analysis. Except for the fact that the analytical samples did not contain benzene molecules of solvation, the results of these analyses are consistent with the crystal structures. The IR spectra of the lanthanacarboranes all showed multiple B–H stretching vibrations in the 2300 – 2500 cm⁻¹ range, which would be expected for complexes that contain Li–H–B bridging structures.^{1,5} Although the paramagnetism of the compounds **2**–**5** precluded the collection of useful NMR data, the rapid relaxation time for samarium did allow compound **1** to be characterized by ¹H, ¹¹B, ⁷Li, and ¹³C NMR spectroscopy. The ¹H NMR spectrum of **1** showed signals due to the CH_2 and CH_3 groups of TMEDA and a single resonance for the CH_3 protons of the SiMe_3 groups,

having about the same chemical shifts as were found in the precursor dilithiacarborane.⁵ In addition, the peak at δ -1.2 ppm found in the ⁷Li NMR of **1** is very close to the value of δ -1.60 ppm reported for the exopolyhedral lithium in the spectrum of the dilithiacarborane.⁵ The crystal structure of **1**, which is similar to that given in Figure 1, shows two different lithium atoms, TMEDA molecules, and SiMe₃ groups; however, their respective NMR spectra do not reflect these differences. At this point it is not known whether some isomerization process leads to the equilibration of these groups in solution or if the broadness of the spectra simply mask any small changes in chemical shifts that would result from the slightly different chemical environments of these groups. The most substantial changes are found when the ¹¹B NMR spectra of **1** are compared with those of either the dilithiacarborane precursor or the trinuclear samaracarborane.¹ The ¹¹B NMR spectrum of compound **1** shows three resonances at δ 13.7, -2.8, and -21.6 ppm, with peak area ratios of 2:1:1, which can be ascribed to B(13,15), B(14), and B(16), respectively (see Figure 1). The dilithiacarborane shows the same 2:1:1 peak area pattern, but at chemical shifts of δ 18.16, 3.18, and -48.40 ppm.⁵ The large deshielding of the apical boron, B(16) in Figure 1, on replacement of a group 1 metal with some other metal is a common feature of this carborane system.¹⁷ The apical boron chemical shifts have been qualitatively explained by noting that the capping metal and the apical boron compete for electron density in the C₂B₃ bonding face and that any strengthening of the metal–carborane interactions will tend to drain electron density away from the apical boron, resulting in an upfield shift in its resonance.¹⁸ Therefore, the change from δ -48.40 to -21.6 ppm found on replacement of a lithium with a trivalent Ln(III) ion is not surprising. However, it should be pointed out that factors other than gross electron density have been found to be important in determining ¹¹B NMR chemical shifts.¹⁹ In this regard it should also be pointed out that the ¹¹B NMR spectrum of the trinuclear half-sandwich samaracarborane cluster shows resonances at δ 20.25, 7.47, 0.76, and -17.6 ppm, with peak area ratios of 1:1:1:1,¹ which is quite different from that found for either **1** or the dilithiacarborane. These differences are not easily explained on the basis of simple electron distribution arguments.

EPR Spectra. Two of the compounds, the gadolinium complex (**2**) and the dysprosium complex (**3**), were studied by EPR spectroscopy. The dysprosium complex was found to be EPR-silent at 3.5 K both in the solid state and in frozen toluene, which can be attributed to the very rapid EPR relaxation of the presumed ⁶H_{15/2} ground state of the metal. On the other

(17) (a) Maguire, J. A.; Fagner, J. S.; Siriwardane, U.; Banewicz, J. J.; Hosmane, N. S. *Struct. Chem.* **1990**, *1*, 583. (b) Zhang, H.; Wang, Y.; Saxena, A. K.; Oki, A. R.; Maguire, J. A.; Hosmane, N. S. *Organometallics* **1993**, *12*, 3933.

(18) Maguire, J. A.; Ford, G. P.; Hosmane, N. S. *Inorg. Chem.* **1988**, *27*, 3354.

(19) (a) Hermánek, S.; Hnyk, D.; Havlas, Z. *J. Chem. Soc., Chem. Commun.* **1989**, 1859. (b) Bühl, M.; Schleyer, P. v. R.; Havlas, Z.; Hnyk, D.; Hermánek, S. *Inorg. Chem.* **1991**, *30*, 3107. (c) Fehlner, T. P.; Czech, P. T.; Fenske, R. F. *Inorg. Chem.* **1990**, *29*, 3103.

hand, in frozen toluene glass, the gadolinium compound (**2**) exhibited an extensively structured EPR signal between 0 and 700 mT (not shown). Such a signal would be expected for the ⁸S_{7/2} ground state of Gd³⁺, which is known for its relatively slow EPR relaxation. Because of the unsymmetrical environment of the Gd³⁺ center and the random orientation of the spins in the frozen solution, no attempt was made to analyze the spectrum of **2**.

Magnetic Susceptibilities. The molar magnetic susceptibilities of compounds **1**–**4** followed the Curie–Weiss law, $\chi = C/(T - \Theta)$ with $\Theta \approx 0$ K, indicating only very weak magnetic interactions. The Curie constants, *C*, correspond to effective magnetic moments of 7.3, 9.4, and 10.1 μ_B per atom for Gd, Dy, and Ho, respectively. The results indicate that crystal field effects play little or no role in the temperature range studied and that free ion behavior can be safely assumed. This was the same conclusion reached earlier for the Er complex (**5**).^{14a} The samaracarborane **1** exhibited a temperature-dependent effective magnetic moment, with a room-temperature value of 1.1 μ_B per Sm atom. This is slightly higher than the expected Sm³⁺ free ion value for $J = 5/2$ and can be attributed to an admixture of the close-by $J = 7/2$ state.

Conclusions

Unlike the results found in the presence of THF, the reaction of the TMEDA-solvated dilithiacarboranes with a number of LnCl₃ salts, in the absence of oxygen-containing compounds, produced bent-sandwich complexes of the general form {Ln(Cl)₂[η^5 -(SiMe₃)₂C₂B₄-H₄]₂}³⁻. These are the expected products from such a reaction scheme, and all have structures that are similar to those found in the lanthanide sandwich compounds of the cyclopentadienide¹⁵ and the larger C₂B₉ cage systems.^{10–12} These results indicate that in the syntheses of the lanthanacarboranes the complete reaction environment must be considered, including the nature of supposedly nonparticipating solvating molecules.

Acknowledgment. This work was supported in part by grants from the Texas Advanced Technology Program (Grant No. 003613006), the National Science Foundation (Grant No. CHE-9400672), the Robert A. Welch Foundation (Grant No. N-1016), and the donors of the Petroleum Research Fund, administered by the American Chemical Society.

Supporting Information Available: Perspective views of the structures of **1**, **3**, **4**, and **5** (Figures S-1–S-4), selected bond lengths and bond angles (Tables S-1 and S-2 for **1**, Tables S-5 and S-6 for **2**, Tables S-9 and S-10 for **3**, Tables S-13 and S-14 for **4**, and Tables S-17 and S-18 for **5**), anisotropic displacement parameters (Tables S-3, S-7, S-11, S-15, and S-19 for **1**–**5**, respectively), and H atom coordinates and isotropic displacement coefficients (Tables S-4, S-8, S-12, S-16, and S-20 for **1**–**5**, respectively) (44 pages). Ordering information is given on any current masthead page.

OM950780Y